Piotr Śliwiński, Marek St. Węglowski, Krzysztof Kwieciński

Electron Beam Welding – Dissimilar Joints of Steels and Nickel Alloys

Abstract: Because of differences in physical and chemical properties of materials being joined as well as due to phenomena such as the formation of intermetallic phases, the making of dissimilar joints poses significant problems for the welding industry. Owing to its high power density, achievable high welding rates and the possibility of obtaining high metallurgical purity, electron beam welding is one of the most suitable methods enabling the reduction of adverse phenomena taking place during the welding of dissimilar joints. The research work discussed in the paper involved the making of joints using steel grades 25HM and 304 with nickel alloy (Inconel 600) and the performance of metallographic tests, tensile tests, bend test and hardness measurements. The electron beam welding method used to the make welded joints discussed in the paper meets the criteria specified in the PN-EN ISO 15614-11 standard.

Keywords: dissimilar joints, intermetallic phases, the electron beam welding method

DOI: 10.17729/ebis.2023.3/2

Introduction

Present-day solutions increasingly often require the fabrication of joints made of materials characterised by significantly varying physicochemical solutions. Demand for dissimilar joints is typical of the power, shipbuilding, aviation, space and defence industries as well as in railway engineering. Dissimilar joints are applied to reduce the cost of materials and the weight of elements as well as to improve operational properties and increase resistance to adverse environmental conditions [1–2].

Typically, dissimilar joints include joints of structural unalloyed steels with corrosion-resistant steels and/or with nickel alloys. The joining of materials characterised by significantly varying physicochemical properties poses numerous problems. Maladjusted process parameters can lead to the formation of joints whose properties may preclude the practical application of the former. Major problems accompanying the fabrication of dissimilar joints include the formation of brittle intermetallic phases, the limited intersolubility of chemical elements as well as varying melting points, thermal expansion coefficients or thermal conductivity and galvanic corrosion-related problems or susceptibility to cracking [1–4].

Because of its characteristics, a method, which enables the obtainment of high-quality similar and dissimilar joints is electron beam welding. Although the aforesaid technology has been industrially applied for many years (as the welding heat source), it continues to develop dynamically both in terms of research and industrial practice [3–6].

Depending on the geometry of the focused electron beam and an electron gun operating mode (stationary or oscillating beam) it is possible to modify a heat input (within a wide range) and the dilution of materials, which enables the joining of elements made of dissimilar metallic materials or alloys and of various thicknesses and shapes. The performance of the joining process under vacuum conditions enables the obtainment of joints characterised by very high metallurgic purity. Electron beam welding provides both the high quality of welded joints and the high efficiency of the joining process [3–6].

mgr inż. Piotr Śliwiński, dr inż. Marek St. Węglowski, mgr inż. Krzysztof Kwieciński – Sieć Badawcza Łukasiewicz – Górnośląski Instytut Technologiczny, Centrum Spawalnictwa, Grupa Badawcza Spawalność i Konstrukcje Spawane (Łukasiewicz Research Network – Upper Silesian Institute of Technology – Welding Centre, Research Group for Materials Weldability and Welded Structures)

Overview of reference publications

Welded joints made of steels and nickel alloys belong to the best tested types of dissimilar joints as they have been commonly used in the power industry for decades [8]. Joints of certain nickel alloys and high-strength structural steels are also applied in the aviation and space industries [9]. The use of dissimilar welds helps reduce costs of components and obtain more favourable properties of structures exposed to high temperature, high pressure and corrosive environments. Because of conditions accompanying construction or repair works performed in power systems, the most common methods applied to join structures are arc-based processes (e.g. direct joining of two materials involving the use of a nickel alloy-based filler metal (e.g. Inconel 82 and 182) or prefabricated bimetallic elements). Table 1 presents the comparison of the primary properties of nickel and iron.

Table 1. Primary properties of nickel and iron [10, 11]

Parameter	Nickel	Iron
Ionisation energy, eV	7.60	7.80
Melting heat, $J \cdot kg^{-1}$	$1.7 \cdot 10^5$	$2.7 \cdot 10^5$
Melting point, °C	1455.00	1536.00
Boling point, °C	2730.00	2860.00
Thermal conductivity, $W \cdot m^{-1} \cdot K^{-1}$	90.90	80.00
Thermal expansion coefficient, K^{-1}	$13.4 \cdot 10^{-6}$	$11 \cdot 10^{-6}$
Density, $kg \cdot m^{-3}$	8908.00	7870.00
Coefficient of elasticity, GPa	200.00	210.00
Resistivity, μΩ·m	0.0693	1.386

Researchers state that general issues concerning dissimilar joints are related to post-weld stresses, creep resistance, ageing as well as structural changes occurring in the weld and in the heat affected zone (HAZ). In addition, intermetallic compounds of iron and nickel (e.g. Fe_3Ni, FeNi and $FeNi_3$ – see Fig. 1) as well as of other chemical elements formed (in the weld) in the transition zone between metals affect plasticity and susceptibility to cracking and corrosion. Cracking processes triggered by the creep of the metal in joints [8, 12–16] or by corrosion [17, 18] usually take place along grain boundaries, i.e. between the weld and the HAZ (on the steel side). For this reason, particular attention should be paid to the above-named areas when testing mechanical properties and the corrosion resistance of such joints.

In dissimilar joints containing materials of various crystalline structures (as is the case with joining ferritic steels with austenitic nickel alloys), wetting between the base material and the liquid weld metal is not as good as in similar joints. The nucleation of the weld metal is heterogonous and takes place on the partially melted grain of the heat affected zone (HAZ). Because of such a manner of crystallisation, crystal nuclei may not be characterised by preferred orientations (as is the case with similar joints). As a result, the fusion line is characterised by random disorientation between grains of the base material and those of the weld. The foregoing is significant importance in terms of subsequent transformations during the cooling process, particularly as regards the formation of type II boundaries (favouring crack formation).

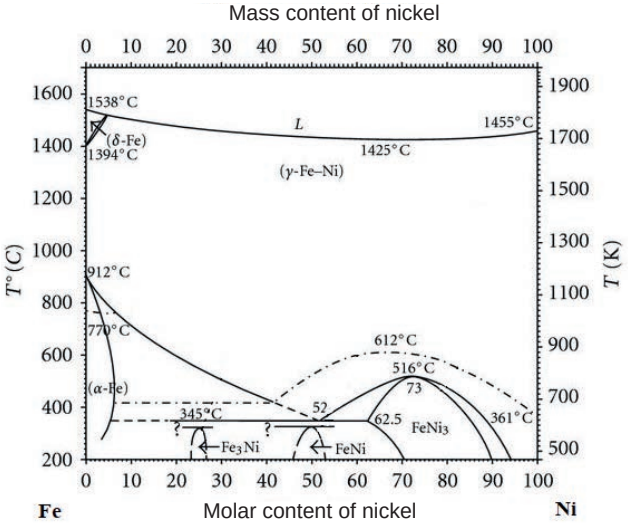

Fig. 1. Diagram of the Fe-Ni phase equilibrium [19]

Unlike type I boundaries, type II boundaries are parallel in relation to the fusion line, usually less than 100 μm deep inside the weld. As mentioned above, such an orientation of crystallites results from differences in the crystalline structure between materials. Cracking in dissimilar joints usually takes place near the fusion line, along the transition zone of martensite (adjacent to the fusion line) as well as along type II boundary in the weld material.

Similar to the welding of similar joints, during the welding of ferritic steels characterised by high susceptibility to cracking the application of preheating may help reduce an increase in HAZ hardness. The heat treatment [20] of dissimilar joints may provide beneficial results including the elimination of stresses present in the material, the homogenisation of the chemical composition of the weld and, in cases where one of the materials is

ferritic steel characterised by susceptibility to hardening, the tempering of the steel.

Figure 2 presents an exemplary microstructure of a welded joint made of steel grade X60 and alloy Inconel 625 with the filler metal (also Inconel 625).

Because of its limitations, the electron beam welding of dissimilar joints made of steels and nickel alloys can be applied to make bimetallic prefabricated products easily joinable using other methods. Welds made using the EBW method are characterised by a narrow width in comparison with their height. In addition, the electron beam welding process makes it possible to decrease the number of beads when welding thicker elements and reduce the phenomenon of hot cracking (because of low linear energy).

The authors of work [18] investigated the corrosion-resistance of a joint made of alloy Inconel 617 and corrosion-resistant steel AISI 310. The use of the EBW process triggered the segregation of chemical elements in the weld and led to the formation of precipitates in interdendritic areas. The weld was characterised by lower corrosion resistance and resistance to pitting corrosion than those of base materials. Such a situation was induced by the formation of precipitates in the weld, i.e. the areas where corrosion defects were initiated. An increase in the welding rate was accompanied by the improvement of corrosion resistance (including resistance to pitting corrosion), which resulted from the formation of the finer dendritic microstructure.

The authors of publication [21] demonstrated that the EBW technology can be used to weld 50 mm thick elements made of cast steel CB2 and nickel alloy-based cast (A625) without preheating and post-weld heat treatment. The adjustment of appropriate welding parameters enabled the obtainment of full penetration and favourable mechanical properties of the joint. Microstructural and strength-related tests revealed the satisfaction of all quality-related requirements concerning the microstructure of the weld and its mechanical properties. A very thin layer characterised by higher hardness (located in the HAZ, on the side of cast steel CB2) did not significantly affect

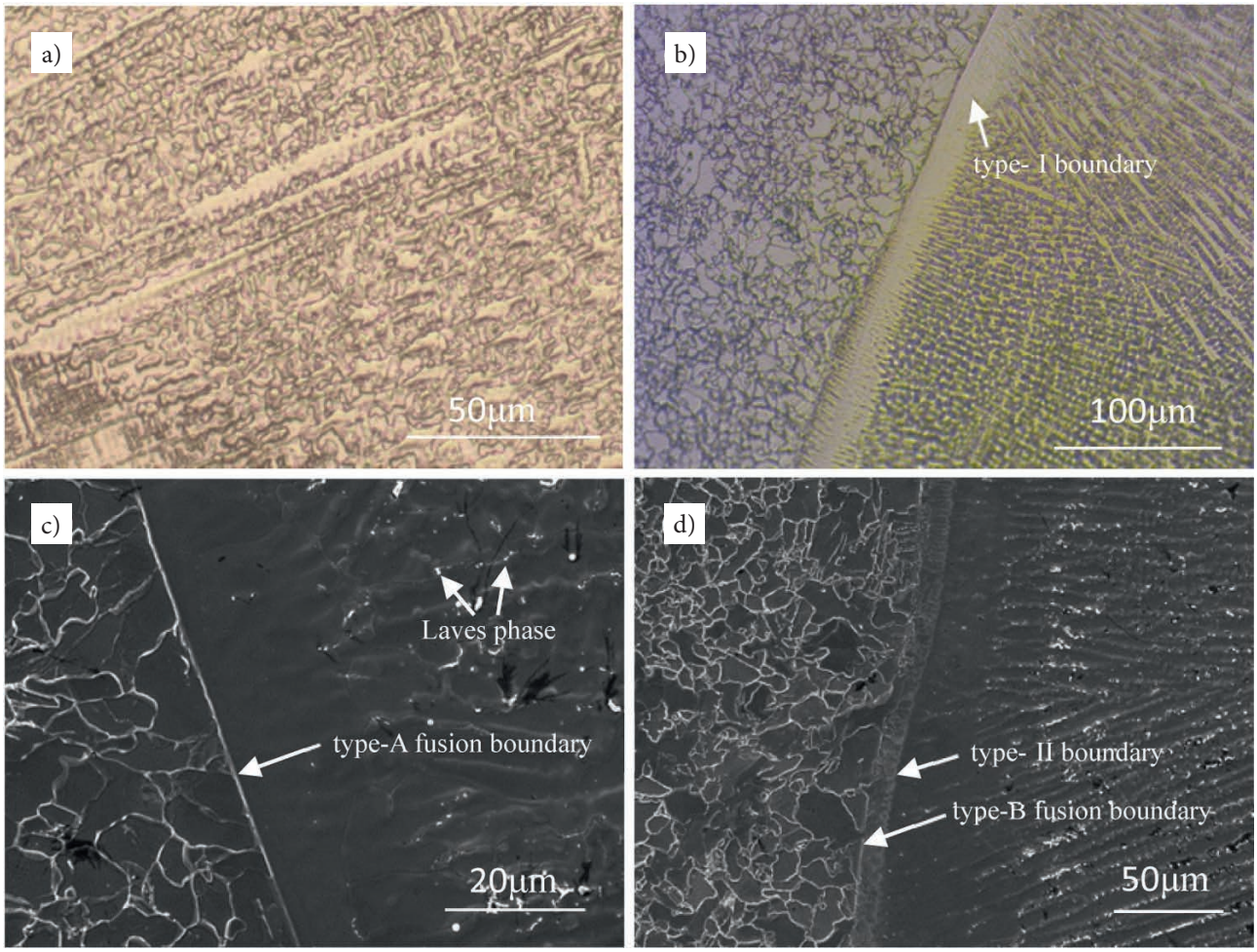

Fig. 2. Microstructures of dissimilar joints made of pipeline steel X60 and Inconel 625: a) microstructure of the weld made using filler metal Inconel 625, b) fusion line and c) and d) SEM photographs of the fusion line [17]

the mechanical properties of the joint. The tensile strength of the specimen subjected to heat treatment amounted to 551 MPa, whereas that of the specimen not subjected to heat treatment amounted to 524 MPa. Figure 3 presents the cross-section of the electron beam welded joint and that of the joint obtained using the MMAW method. The distribution of hardness in the specimens is presented in Figure 4.

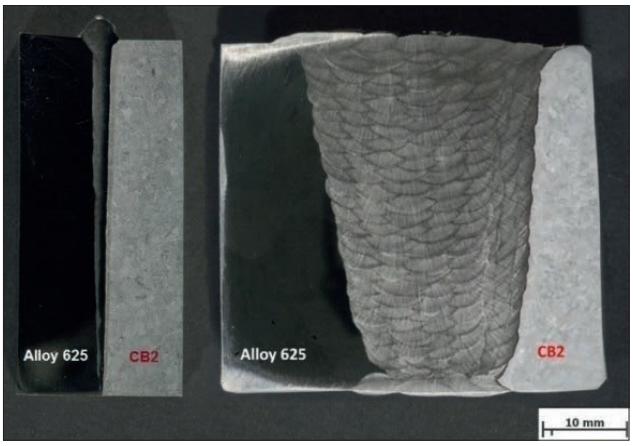

Fig. 3. Electron beam welded joint (left) and the joint obtained using the MMAW process (right) [21]

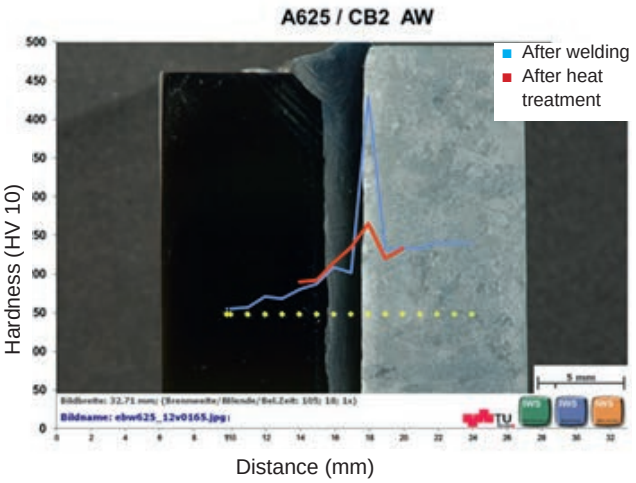

Fig. 4. Hardness distribution in the electron beam welded joint before and after heat treatment [21]

Publication [22] presents results of tests involving dissimilar joints made of corrosion-resistant duplex steel grade UNS S32205 and alloy Inconel 625 using the electron beam welding process. The joints obtained in the tests were free from imperfections, their tensile strength amounted to 850 MPa, whereas the rupture took place in the weld. The joints did not reveal any increase in hardness. The heat affected zones were not characterised by significant grain refinement or any other negative metallurgical effects. The tensile tests confirmed that damage was located in the weld zone, which was primarily because of the segregation of phases rich in molybdenum. The toughness of the welds was lower in comparison with the values typical of the base materials. Figure 5 presents the cross-section of the joint.

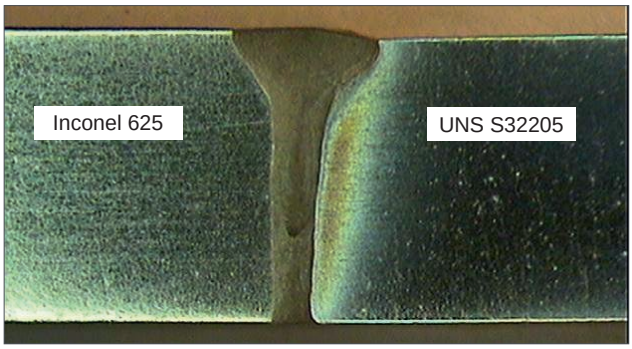

Fig. 5. Cross-section of the joint made of steel grade UNS S32205 and alloy Inconel 625 [22]

The electron beam welding [23] of joints made of alloy Inconel 625 and steel grade AISI 304L using optimised process parameters enabled the obtainment of a homogenous joint characterised by full penetration and the uniform distribution of chemical elements in the weld. The area near the terminal crater contained a few microcracks along dendrite boundaries, which was primarily caused by the segregation of sulphur compounds in those areas. Cross-sectional microhardness measurements revealed that the hardness in the weld tended to increase on the side of steel grade AISI 304L, towards base alloy Inconel 625.

Tests and results

Welding and braze welding processes were performed at the Welding Centre of the Upper Silesian Institute of Technology (of the Łukasiewicz Research Network) using a CVE EB 756 system (Cambridge Vacuum Engineering). Macro and microstructural tests were performed using an Eclipse MA200 light microscope (Nikon) provided with a DS-Fi2 digital camera (Nikon). Vickers hardness tests were performed using an automated hardness tester (KB Prüftechnik).

The method applied to join steel with nickel alloys was butt welding without the use of the filler metal.

Plates made of steel grades 304 25HM (80 mm × 200 mm) were put together in the butt configuration with plates made of alloy Inconel 600 using a special positioning grip ensuring the proper clamp of the plates to be joined (Fig. 6).

Fig. 6. Positioning grip fixed on the work table of the electron beam welding machine

The first stage, aimed at the initial adjustment of process parameters, involved the melting of sheets made of steel grades 25HM and 304 as well as of nickel alloy Inconel 600. The accelerating voltage amounted to 120 kV, the focal length amounted to 420 mm (the beam being focused on the surface), whereas the pressure in the working chamber amounted to 1×10^{-4}. Variable process parameters were the travel rate (restricted within the range of 500 mm/min to 2000 mm/min) and the beam current (restricted within the range of 5 mA to 20 mA). The visual inspection of penetrations led to the narrowing of the range of parameters used when making test joints.

The subsequent stage involved the welding of the plates using configurations and parameters presented in Table 2. Before welding, joints 1 through 8 were preheated to a temperature of 250°C using the oscillating debunched electron beam.

Figures 7–12 present cross-sections of dissimilar welded joints along with photographs of microstructures in designated joint areas and hardness distribution. The test specimens were subjected to grinding, polishing and etching in Nital (steel 25HM) and/or electrolytic etching in the aqueous solution of nitric acid (40 : 60 HNO_3 : H_2O – steel 304 and nickel alloy).

The tensile tests were performed in accordance with the requirements specified in the PN-EN ISO 4136:2022-12 standard [24], whereas the bend tests were performed in accordance with the requirements of the PN-EN ISO 5173:2010/A1:2012 standard [25]. The test results are presented in Table 3.

Analysis of test results

The microstructure of steel grade 25HM contained ferrite and pearlite, whereas the microstructure of welded joint 1 was composed primarily of martensite in the weld and in the HAZ near the fusion line as well as of the mixture of martensite and ferrite in the HAZ, deep inside the base material. The similar structure was observed in the HAZ of joints 7, 8 and 9. An increase in the welding rate (joint 7: 500 mm/min and joint 9: 1000 mm/min) without preheating resulted in a significant hardness increase

Table 2. Parameters used in the welding of the Fe-Ni joints

Specimen no.	Materials used	Accelerating voltage, kV	Beam current, mA	Work table travel rate, mm/min	Focal length, mm	Pressure in the chamber, mbar
1	25HM	120	7	500	420	$1\cdot10^{-4}$
2	600	120	12	1000	420	$1\cdot10^{-4}$
3	304	120	12	1000	420	$1\cdot10^{-4}$
4	304-600	120	8	500	420	$1\cdot10^{-4}$
5	304-600	120	12.5	1000	420	$1\cdot10^{-4}$
6	304-600	120	16	2000	420	$1\cdot10^{-4}$
7	25HM-600	120	8	500	420	$1\cdot10^{-4}$
8	25HM-600	120	7	500	420	$1\cdot10^{-4}$
9	25HM-600	120	11.5	1000	420	$1\cdot10^{-4}$

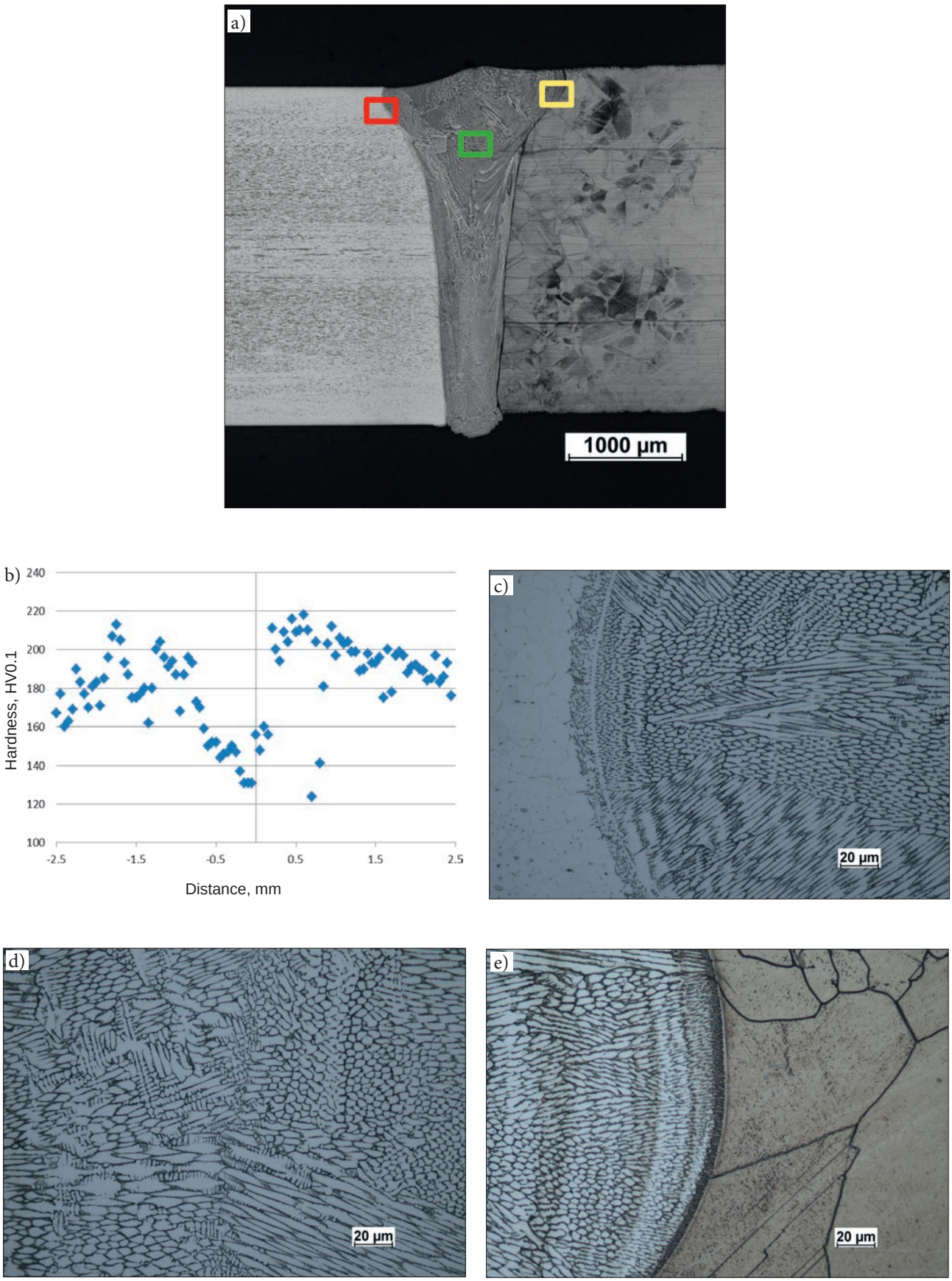

Fig. 7. Joint 4 (304-600): a) joint cross section, b) hardness distribution in the joint, c) microstructure of the HAZ of steel 304, d) microstructure of the weld and e) microstructure of the HAZ of nickel alloy Inconel 600

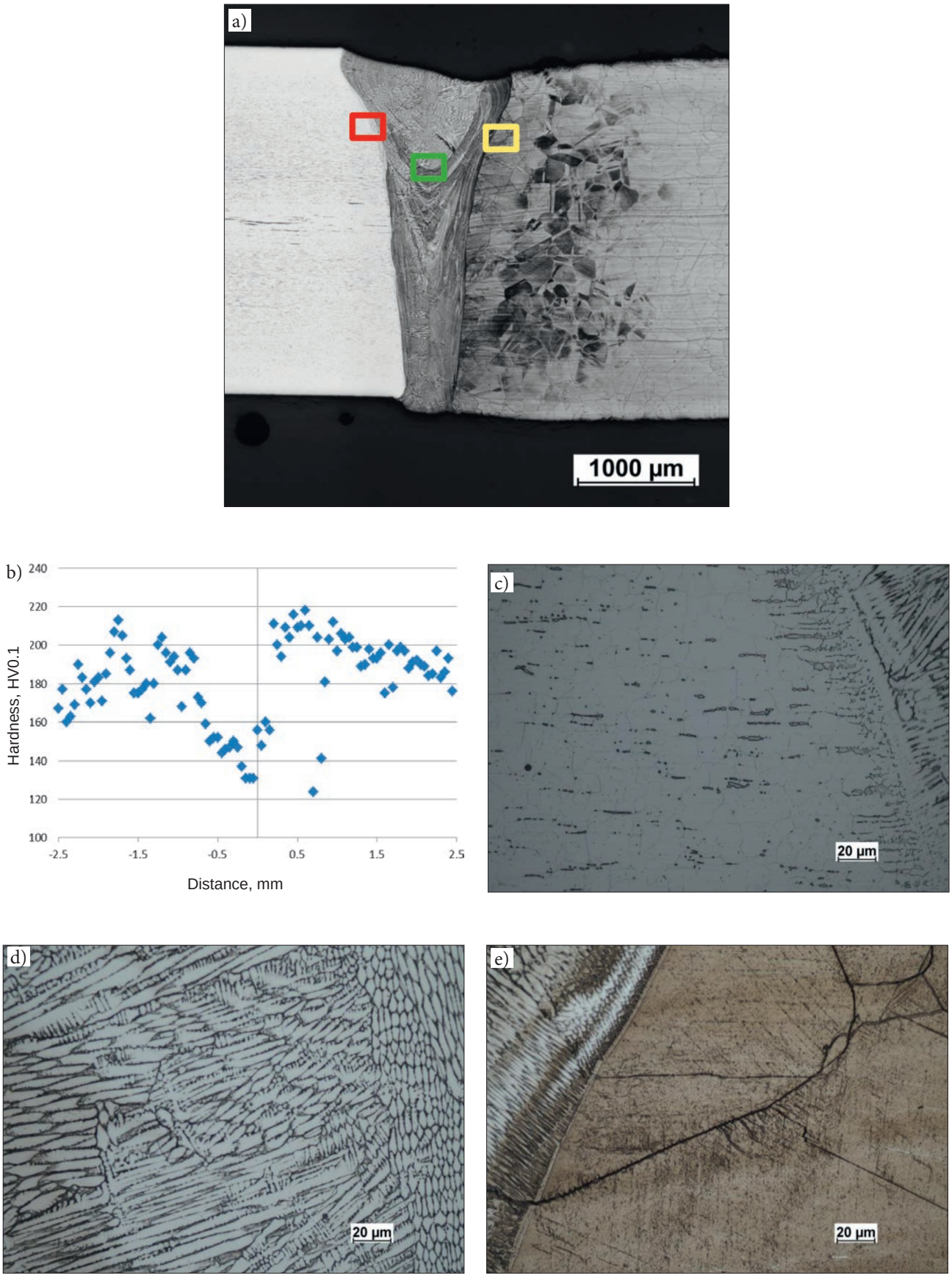

Fig. 8. Joint 5 (304-600): a) joint cross section, b) hardness distribution in the joint, c) microstructure of the HAZ of steel 304, d) microstructure of the weld and e) microstructure of the HAZ of nickel alloy Inconel 600

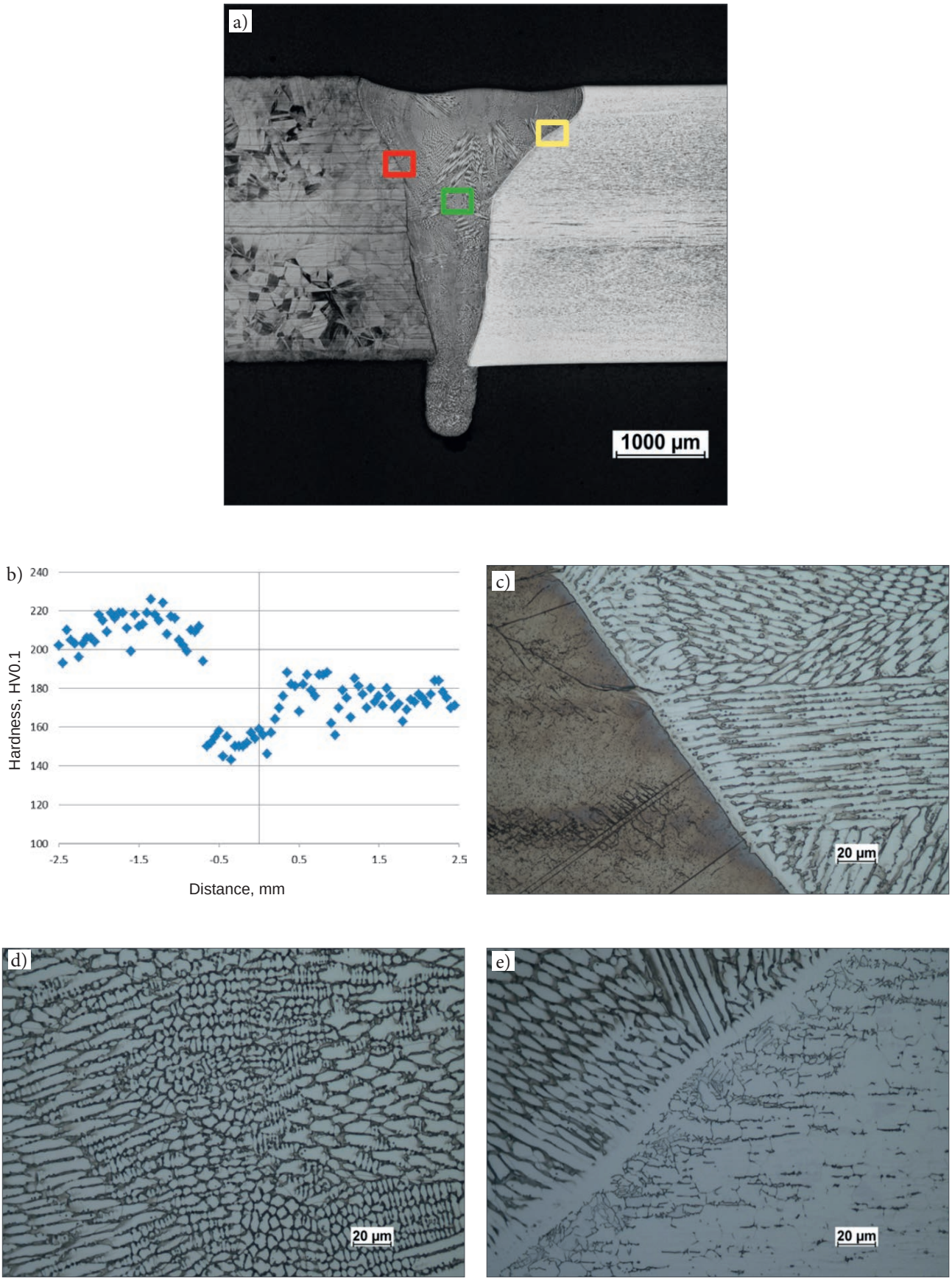

Fig. 9. Joint 6 (304-600): a) joint cross section, b) hardness distribution in the joint, c) microstructure of the HAZ of nickel alloy Inconel 600, d) microstructure of the weld and e) microstructure of the HAZ of steel 304

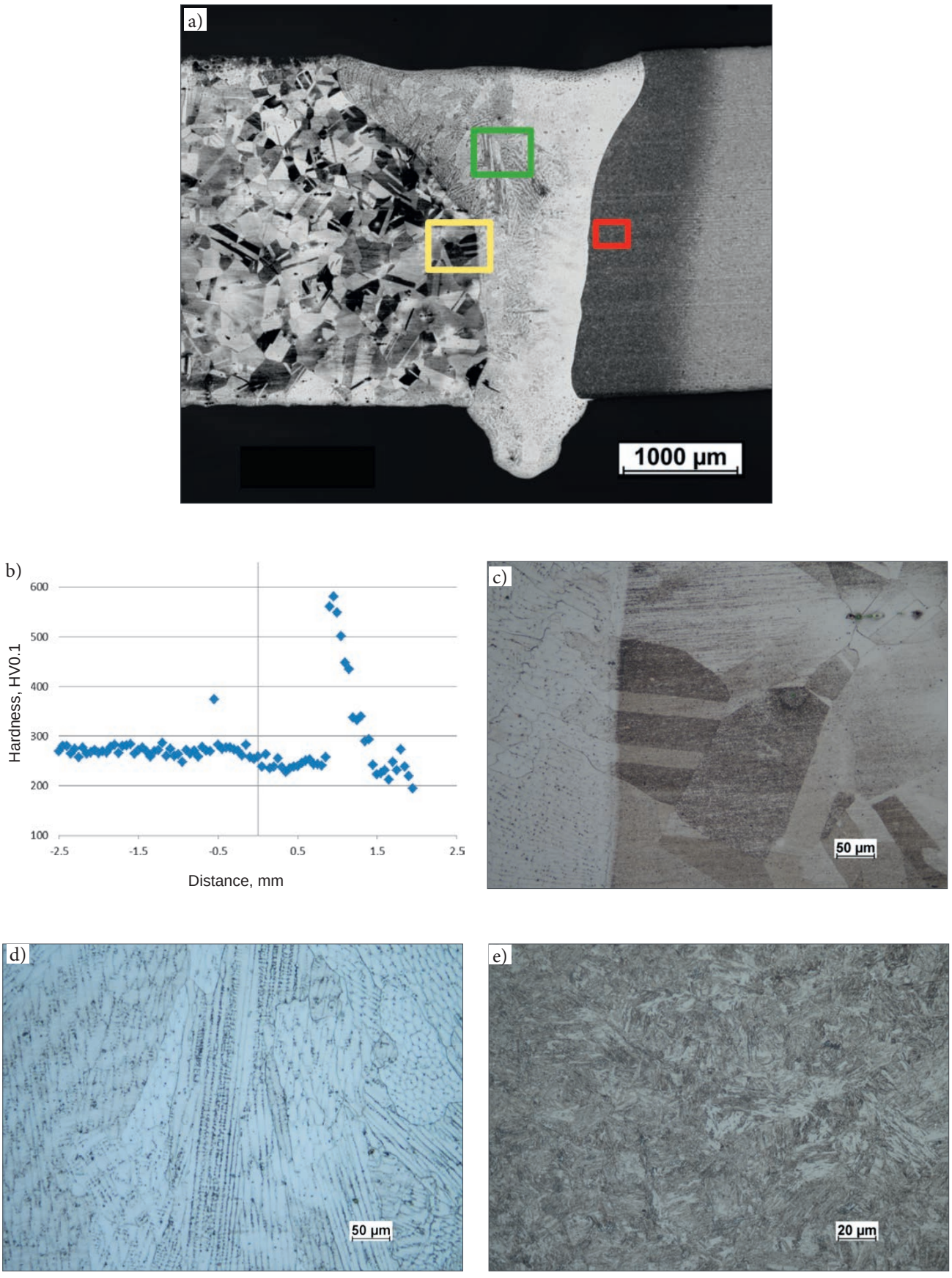

Fig. 10. Joint 7 (600-25HM): a) joint cross section (view inverted horizontally), b) hardness distribution in the joint, c) microstructure of the HAZ of nickel alloy Inconel 600, d) microstructure of the weld and e) microstructure of the HAZ of steel 25HM

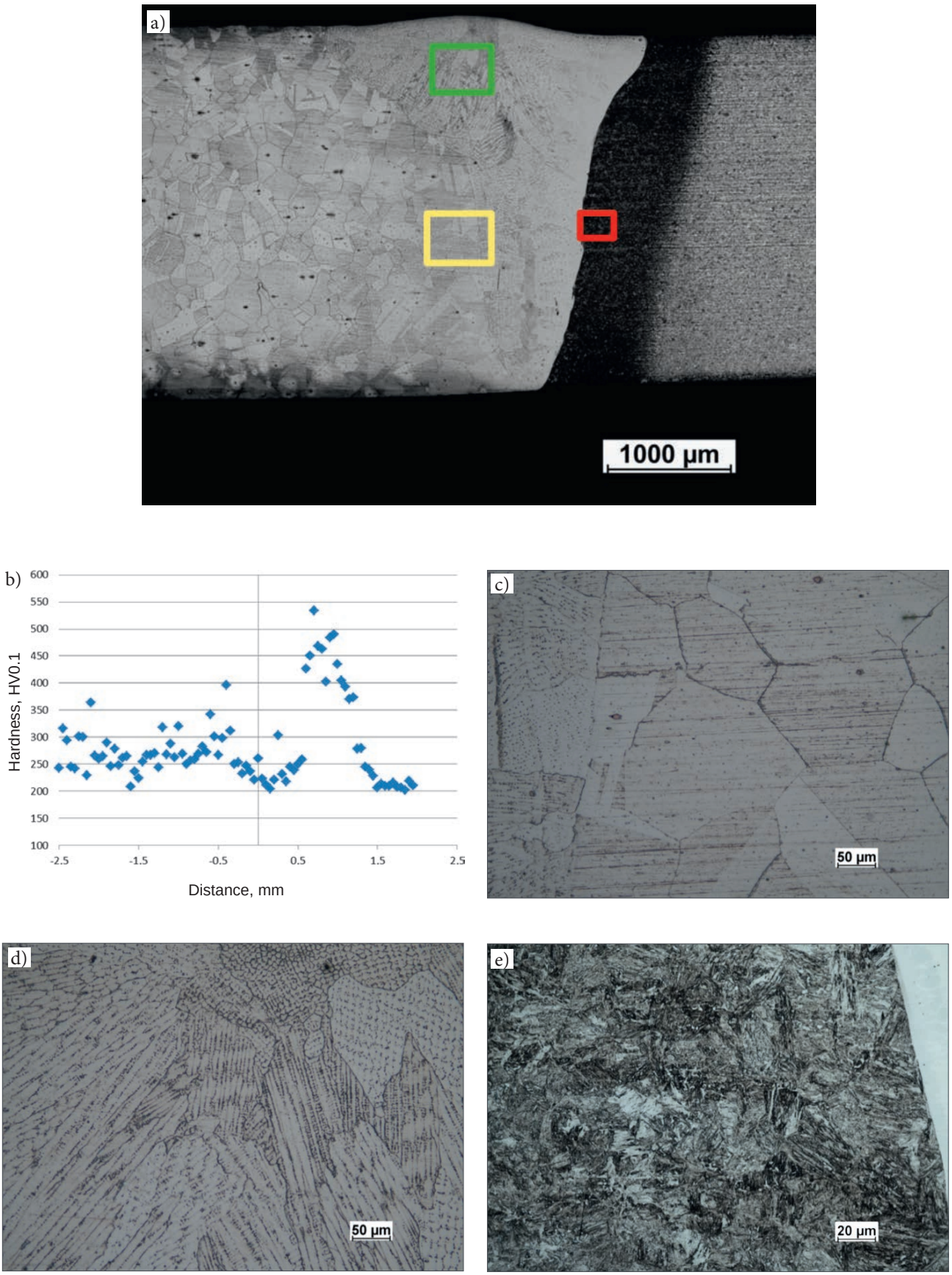

Fig. 11. Joint 8 (600-25HM): a) joint cross section (view inverted horizontally), b) hardness distribution in the joint, c) microstructure of the HAZ of nickel alloy Inconel 600, d) microstructure of the weld and e) microstructure of the HAZ of steel 25HM

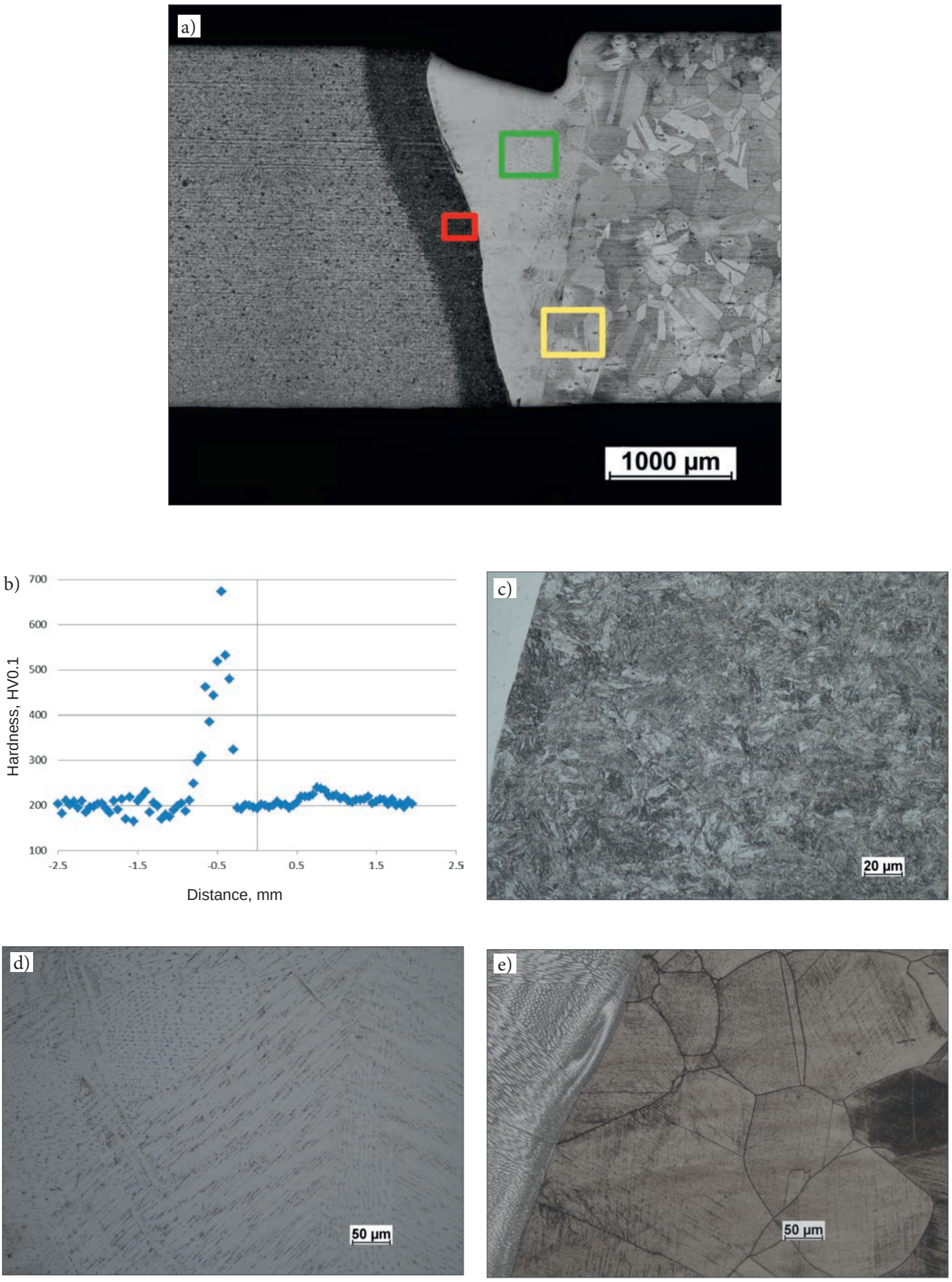

Fig. 12. Joint 9 (25HM-600): a) joint cross section, b) hardness distribution in the joint, c) microstructure of the HAZ of steel 25HM, d) microstructure of the weld and e) microstructure of the HAZ of nickel alloy Inconel 600

Table 3. Mechanical test results concerning the Fe-Ni welded joints

Joint no.	Material of the joint	Average tensile strength, MPa	Did the rupture take place in the weld?	Bend test	Bending pin diameter, mm	Max. hardness, HV0.1
1	25HM	531.7	NO	No cracks	15	515
2	600	654.6	YES	No cracks	10	202
3	304	703.3	YES	No cracks	10	213
4	304-600	611.0	YES	No cracks	10	211
5	304-600	576.1	YES	No cracks	10	219
6	304-600	521.7	YES	No cracks	10	226
7	25HM-600	544.3	NO	No cracks	15	581
8	25HM-600	542.8	NO	No cracks	15	534
9	25HM-600	542.0	NO	No cracks	15	673

of 92 HV0.1. In turn, the application of preheating up to a temperature of 250°C (in relation to joint 8, welded at a rate of 500 mm/min) reduced the maximum hardness by 47 HV0.1. The preheating temperature and the welding rate did not affect the tensile strength of the dissimilar joints made of steel 25HM and nickel alloy Inconel 600. Because of the high content of nickel from alloy Inconel 600, the weld of the dissimilar joints (25HM-600) was characterised by the austenitic structure. The welds were characterised by the columnar-dendritic structure and a low hardness of approximately 250 HV0.1. The significant difference between the hardness in the HAZ of steel grade 25HM and the material of the austenitic weld (approximately 300 HV0.1) led to the formation of a structural notch.

Because both steel grade 304 and nickel alloy Inconel 600 have the austenitic structure, the dissimilar joints of the above-named alloys were also characterised by the above-named type of structure. In the similar joint made of steel grade 304 as well as the dissimilar joints involving the nickel alloy, in the HAZ|, near the fusion line, on the side of the steel it was possible to observe significant amounts of ferrite δ (visible as the lattice of irregular dark precipitates). At higher temperature, the presence of ferrite delta could trigger the formation of brittle phase σ, the presence of which negatively affects the strength of joints. An increase in the welding rate (joint 4: 500 mm/min, joint 5: 1000 mm/min and joint 6: 2000 mm/min) was accompanied by an increase in the maximum measured hardness and a decrease in average tensile strength. The bend tests of the specimens sampled from joint 4 led to the formation of weld face cracks. The distribution of hardness in the dissimilar joints made of steel grade 304 and nickel alloy Inconel 600 was uniform. The nickel alloy was characterised by hardness restricted within the range of approximately 200 HV0.1 to 230 HV0.1, whereas the hardness of steel grade 304 amounted to approximately 170 HV0.1. The hardness in the weld was lower and restricted within the range of 130 HV0.1 to 160 HV0.1.

Conclusions

The above-presented tests and results led to the formulation of the following conclusions:

- The electron beam welding technology enables the obtainment of joints made of steels and nickel alloys and characterised by satisfactory properties.
- The joints made of steel grades 25HM and 304 and of nickel alloy Inconel 600 were characterised by high tensile strength and satisfied qualification requirements in accordance with the PN-EN ISO 15614-11 standard [26].
- The welding of steel 25HM triggered a high increase in hardness in the HAZ areas of the joints, yet, during the tensile test, the rupture took place in the base material, on the side of the steel. The bend tests did not reveal the presence of cracks in the weld face or weld root areas. The structural notch formed during the welding process could adversely affect the fatigue strength of the joints.

Acknowledgements

The above presented tests, performed at the Welding Centre of the Silesian Institute of Technology of the Łukasiewicz Research Network, were financed using s subsidy granted by the Ministry of Science and Higher Education within research work no. Ac-164 (no. ST-12) Investigating the Possibility of the Making of Dissimilar Joints Using the Electron Beam Welding Technology.

References

[1] Martinsen K., Hu S.J., Carlson B.: Joining of dissimilar materials. CIRP Annals – Manufacturing Technology, 2015, vol. 64, no. 2, pp. 679-699.

[2] Kah P., Martikainen M.: Trends in Joining Dissimilar Metals by Welding. Applied Mechanics and Materials, 2013, vol. 440, pp. 269–276.

[3] Metzger G., Lison, R.: Electron beam welding of dissimilar metals. Weld J (Miami), 1976, vol. 55, no. 8, pp. 230–240.

[4] Sun Z., Karppi R.: The application of electron beam welding for the joining of dissimilar metals: an overview. Journal of Materials Processing Technology, 1996, vol. 59, no. 3, pp. 257–267.

[5] Węglowski M.St., Błacha S., Dworak J.: Spawanie wiązką elektronów – charakterystyka metody. Biuletyn Instytutu Spawalnictwa, 2014, vol. 58, no. 3, pp. 25–32.

[6] Volker A., Clauß U. et al.: The fundamentals of a fascinating technology. Wydawnictwo Probeam, 2011.

[7] Casalino G., Guglielmi P., Lorusso V.D., Mortello M., Peyre P., Sorgente D.: Laser offset welding of AZ31B magnesium alloy to 316 stainless steel. Journal of Materials Processing Technology, 2017, vol. 242, pp. 49–59.

[8] Mouginot R., Hänninen H.: Microstructures of nickel-base alloy dissimilar metal welds. Aalto University publication series, vol. Aalto-ST 5/2013, p. 178.

[9] Anuradha M., Chittaranjan Das Vemulapalli, Muralimohan Cheepu: Effect of filler materials on dissimilar TIG welding of Inconel 718 to high strength steel. Materials Today: Proceedings, 2021, vol. 52 no. 6.

[10] Hammond C.R., Lide C.R.: The elements. In Rumble, John R. (ed.). CRC Handbook of Chemistry and Physics (99th ed.), Boca Raton, FL: CRC Press, 2018, p. 4.22. ISBN 9781138561632.

[11] Davis J.R., Mills K.M., Lampman S., Zorc T.B., Lapman H.F., Crankovic G.M., Daquila J.L. (eds.): Metals Handbook: Irons, Steels, and High-Performance Alloys. Properties and Selection. ASM international, 1990.

[12] Maurya A.K., Pandey C., Chhibber R.: Dissimilar welding of duplex stainless steel with Ni alloys: A review. International Journal of Pressure Vessels and Piping, 2021, vol. 192, 104439.

[13] Wang Y., Shao C., Fan M., Ma N., Lu F.: Effect of solidified grain boundary on interfacial creep failure behavior for steel/nickel dissimilar metal welded joint. Materials Science and Engineering: 2021, A, vol. 803, 140482.

[14] Kyeong-Yong S., Ji-Won L., Jung-Min H., Kyong-Woon L., Byeong-Ook K., Hyun-Uk H.: Transition of creep damage region in dissimilar welds between Inconel 740H Ni-based superalloy and P92 ferritic/martensitic steel. Materials Characterization, 2018, vol. 139, pp. 144–152.

[15] Yu Z., Kejian L., Zhipeng C., Jiluan P.: Creep rupture properties of dissimilar metal weld between Inconel 617B and modified 9%Cr martensitic steel. Materials Science and Engineering: A, 2019, vol. 764, 138185.

[16] Yan L., Eskandari Jam J., Heydari Beni M., Javad Kholoud M., Baleanu D., Eskandari Shahrak M., Ghaemi F.: Effect of laser welding parameters on the temperature distribution, microstructure and mechanical properties of dissimilar weld joint of Inconel 625 and stainless steel 304. International Communications in Heat and Mass Transfer, 2022, vol. 131, 105859.

[17] Chengshuang Z., Qiuyan H., Qiang G., Jinyang Z., Xingyang C., Jun Z., Lin Z.: Sulphide stress cracking behaviour of the dissimilar metal welded joint of X60 pipeline steel and Inconel 625 alloy. Corrosion Science, 2016, vol. 110, pp. 242–252.

[18] Derakhshi M.A., Kangazian J., Shamanian M.: Electron beam welding of Inconel 617 to AISI 310: Corrosion behavior of weld metal. Vacuum, 2019, vol. 161, pp. 371–374.

[19] Vernyhora I., Tatarenko V., Bokoch S.: Thermodynamics of f.c.c.-Ni-Fe Alloys in a Static Applied Magnetic Field. ISRN Thermodynamics, 2012, 917836.

[20] Kyoung Joon C., Jong Jin K., Bong Ho L., Chi Bum B., Ji Hyun K.: Effects of thermal aging on microstructures of low alloy steel-Ni base alloy dissimilar metal weld interfaces. Journal of Nuclear Materials, 2013, vol. 441, no. 1–3, pp. 493–502.

[21] Wiednig C., Lochbichler C., Enzinger N., Beal C., Sommitsch C.: Dissimilar Electron Beam Welding of Nickel Base Alloy 625 and 9% Cr Steel. Procedia Engineering, 2014, vol. 86, pp. 184–194.

[22] Devendranath Ramkumar K., Sridhar R., Saurabh Periwal, Smitkumar Oza, Vimal Saxena, Preyas Hidad, Arivazhagan N.: Investigations on the structure – Property relationships of electron beam welded Inconel 625 and UNS 32205. Materials & Design, 2015, vol. 68, pp. 158–166.

[23] Shakil M., Ahmad M., Tariq N.H., Hasan B.A., Akhter J.I., Ahmed E., Mehmood M., Choudhry M.A., Iqbal M.: Microstructure and hardness studies of electron beam welded Inconel 625 and stainless steel 304L. Vacuum, 2014, vol. 110, pp. 121–126.

[24] PN-EN ISO 4136:2022-12 – Badania niszczące złączy spawanych metali – Próba rozciągania próbek poprzecznych.

[25] PN-EN ISO 5173:2010/A1:2012 – Badania niszczące spoin w materiałach metalowych – Badanie na zginanie.

[26] PN-EN ISO 15614-11:2005 – Specyfikacja i kwalifikowanie technologii spawania metali – Badanie technologii spawania – Część 11: Spawanie wiązką elektronów i wiązką promieniowania laserowego.